



Original scientific paper

UDC: 910.27:711.4

<https://doi.org/10.2298/IJGI230822002P>

Received: August 22, 2023

Reviewed: December 12, 2023

Accepted: January 18, 2024



DEVELOPMENT OF GEOSPATIAL PASSABILITY MAPS: A MULTI-CRITERIA ANALYSIS APPROACH

Ivan Potić^{1*}, Marija Stojanović¹, Nina Ćurčić², Dejan Đorđević^{1,3}, Radoje Banković^{1,3}

¹Military Geographical Institute General Stevan Bošković, Belgrade, Serbia; e-mails: ivan.potic@vs.rs; marijasmaki996@gmail.com; dejan.r.djordjevic@vs.rs; radoje.bankovic@vs.rs

²Geographical Institute "Jovan Cvijic" SASA, Belgrade, Serbia; e-mail: n.curcic@gi.sanu.ac.rs

³University of Defence, Military Academy, Belgrade, Serbia

Abstract: This research presents a comprehensive analysis of the production of terrain passability maps in southeastern Serbia, employing a multi-criteria decision-making (MCDM) analysis. The study integrates various geographical and infrastructural aspects, assigning coefficients to each input parameter, including rivers, roads, rails, CORINE Land Cover (CLC), soil, slope, and the Topographic Ruggedness Index (TRI). The introduction of the TRI marks an innovative advancement in terrain analysis and passability. By comparing wet and dry periods, the study provides critical insights into the dynamic nature of terrain passability, with implications for transportation planning and emergency response. The research's innovative approach and detailed examination set it apart, offering valuable contributions to scholarly comprehension and practical applications. The findings underscore the potential for interdisciplinary collaboration and the broad impact of geographic information systems (GIS) and terrain analysis in addressing real-world challenges. Future research may explore additional factors influencing terrain passability and expand the geographical scope of the study.

Keywords: multi-criteria decision-making analysis; geospatial analysis; geographic information systems; geostatistics; terrain modelling

1. Introduction

This research explores terrain passability, focusing on trafficability, which measures a vehicle's ability to traverse specific areas, as defined by Donlon and Kenneth (1999). The study examines the relationship between vehicles and terrain, considering factors such as mathematical transformations for vehicle speed (Donlon & Kenneth, 1999) and the complexity of ground characteristics, including soil conditions (Gumoś, 2005). The concepts have relevance to various fields that heavily rely on passability, such as the military, transportation authorities, urban planners, and environmental conservation efforts.

Ground carrying capacity and soil susceptibility to shearing resistance influence a vehicle's passability. The study also examines traversal over varying soil moisture levels, as proposed by Stevens et al. (2017), and the role of soil mechanics in vehicle performance, as proposed by Dallas

*Corresponding author, e-mail: ivan.potic@vs.rs

et al. (2021), Grabau (1964), and Schulte et al. (2021). Ground conditions, affected by factors like water and topography, are vital in soil development. For instance, the research includes modelling tire-soil interactions (Saarilahti, 2002) and the effects of multiple vehicles traversing specific areas (Gumoś, 2005; House et al., 2001; Okinda et al., 2021).

Land cover, encompassing physical and biological elements like water, vegetation, and rock, is crucial in vehicle passability across various landscapes (Homer et al., 2020; Rybansky, 2022). Different land cover types, such as forests or urban areas, influence vehicle mobility, with certain terrains posing challenges to movement (Rybansky, 2022; Tobler, 1993). The Digital Elevation Model (DEM) and its accuracy are vital in geographic information systems (GIS) and remote sensing, providing details like elevation and slope (Graser et al., 2015; Rada et al., 2021). These factors, affecting traversal difficulty, make DEM essential in predicting and managing terrain-related challenges in transportation planning (Fisher, 1997; Rybansky & Rada, 2022; Wollenstein-Betech et al., 2020).

Developing geospatial passability maps has broad implications in spatial planning, military operations, and crisis management. Historically, tools like the NATO Reference Mobility Model (NRMM) were used, but limitations led to the development of Next-Generation NRMM (NG-NRMM; McCullough et al., 2017). Terrain passability is influenced by geographic factors, classified into levels like Go, Slow Go, and No Go (Rada et al., 2020; Rybanský, 2003). Using GIS to model terrain passability offers insights and applications in planning movements and generating optimal routes, considering passability levels (Dawid & Pokonieczny, 2021; Gumoś, 2005).

The impact of terrain on a vehicle's passability, specifically geographic factors and their characteristics, is a subject of this research. Understanding these factors and their implications on mobility is crucial for enhancing the effectiveness of geospatial passability maps (Rybansky, 2022; Rybansky et al., 2014, 2023). A study by Gigović et al. (2015) proposes a model that combines GIS and multi-criteria techniques to evaluate land manoeuvrability, tested in southern Banat. Another study applies Analytic Hierarchy Process and GIS to urban transport, specifically the City of Setif tramway, demonstrating their efficacy in planning (Djouani et al., 2022). Borisov et al. (2011) utilised GIS to create tank mobility maps, highlighting terrain's role in military operations. Živanović (2015) examined the impact of morphometric parameters on forest fire risks, using GIS to evaluate dangers and intervention possibilities in Golija Nature Park. These studies offer a comprehensive overview of factors influencing terrain passability, forming a foundation for further research in Serbia.

This study introduces advancements in geospatial passability mapping, including the Topographic Ruggedness Index (TRI) and a comparative analysis of wet and dry periods. The study uses a comprehensive multi-criteria decision-making (MCDM) analysis to offer insights into terrain passability with transportation, urban planning, and military operations applications. The methodology underscores the potential for interdisciplinary collaboration and further exploration of terrain passability factors.

2. Materials and methods

The method employed in this study utilises MCDM analysis to generate a final terrain passability grid map. MCDM analysis involves assigning quantitative values to input data through weighted coefficients. Weighted coefficients are assigned to different criteria based on expert knowledge, and sensitivity analysis ensures the robustness of the results. The input data, which are subjected to a Weighted Overlay Analysis (WOA) in the ArcGIS Pro software

(Version 3.1.1; Esri, n.d.-a), encompass a variety of factors. These include the river network, roads and railways, land cover, soil cover, slope, and the TRI (Figure 1).

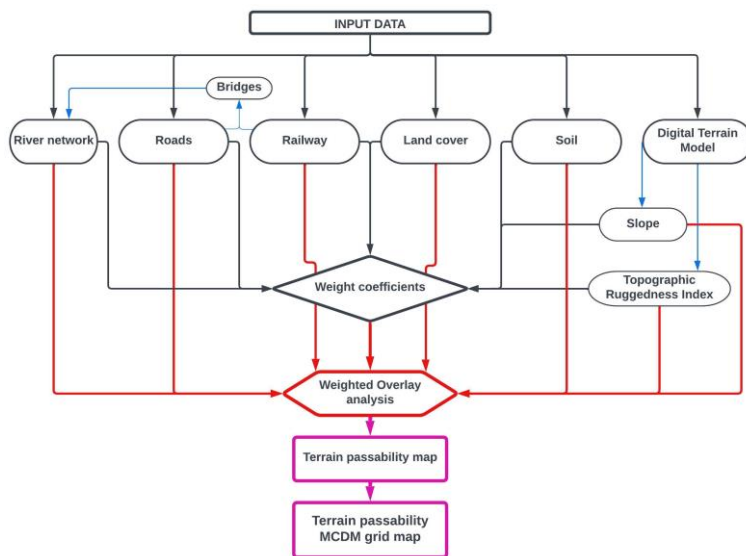


Figure 1. Flow chart illustrating the MCDM process used in the generation of the terrain passability map.

WOA, a GIS-based MCDM analysis method, integrates various information layers for spatial decision-making. In ArcGIS Pro, the Weighted Overlay tool standardizes diverse inputs, assigning weights and summing values to create an output raster (Esri, n.d.-b). The MCDM analysis is applied to wet and dry seasons to understand the differential behaviour of soil types in response to water presence. Increased water saturation may affect soil passability during the wet season, while the absence of water influences soil responses in the dry season. This dual-period analysis enhances the understanding of terrain passability, contributing to a more robust passability map.

2.1. Study area

The study area covers the southeastern part of Serbia, partially extending to the border with Bulgaria. The selected research area falls within the mountain-basin region. The northern part belongs to the Balkan Serbia mesoregion, while the southern part belongs to the Vlasina and Krajište mesoregion (Marković & Pavlović, 1995). The central part of the research area encompasses Greben planina Mountain, Vlaška planina Mountain, and Pirotska kotlina Valley, surrounded by Ruj Mountain to the southwest, Lužnička kotlina Valley and Suva planina Mountain to the east. To the north, the study area extends from Pirotska kotlina Valley to Belava Mountain and Belopalanačka kotlina Valley, while to the east, there is the mountain range of Vidlič (Figure 2). Pirot Region, encompassing the study area, has approximately 76,700 inhabitants, according to the 2022 census data (Statistical Office of the Republic of Serbia, 2023). It includes four settlements: Pirot, Bela Palanka, Babušnica, and Dimitrovgrad. The largest settlement is the city of Pirot, which also serves as the regional centre of this area (Figure 2). The study area covers 2,009.2 km²; the centroid is 43°03'24.615"N, 22°32'02.061"E.

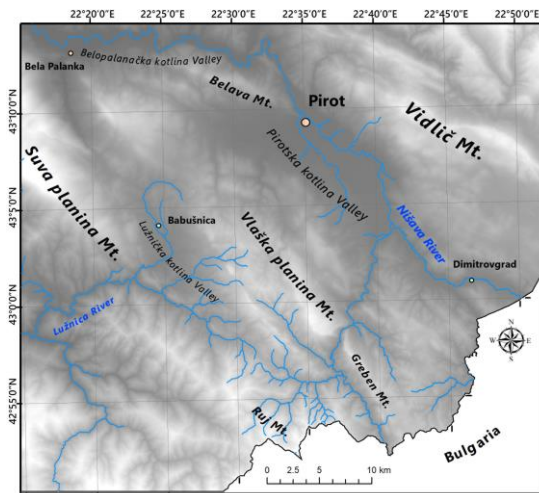


Figure 2. The study area containing a river network.
Note. Data for the study area are obtained and adapted from Planet dump, by OpenStreetMap contributors, 2017 (<https://planet.openstreetmap.org>). CC BY-SA 2.0.

geographic data and mapping and the data are available under the Open Database License (OpenStreetMap contributors, 2017). OpenStreetMap's comprehensive and continually updated database ensures the accuracy and relevance of the data used in this study (OpenStreetMap contributors, 2017).

2.2.2. CORINE Land Cover

The CLC is a pan-European programme that offers information on land cover and changes across Europe (Feranec et al., 2016). It includes land cover and uses classes in a three-level hierarchy, combining observed land cover and socio-economic land use. The standardized methodology, which utilises satellite imagery and ancillary data, enables comparisons over time and space, serving as a valuable tool for environmental policy and various sector applications. The data is adapted from the CLC 2018 (raster 100 m), Europe, 6-yearly - version 2020_20u1, May 2020 dataset (European Environment Agency [EEA] geospatial data catalogue, 2020), which is copyrighted by the EEA (2023).

2.2.3. Soil

The soil data is obtained and adapted employing basic digitalization from the document *Natural Background of Harmful and Dangerous Substances in the Soil of Eastern Serbia* (Institut za zemljište Beograd, 2019) and *Pedological map of SFRY* (Antonović, 1982). These documents provide a wide-ranging outline of the soil characteristics in Eastern Serbia, which is crucial for understanding the potential challenges and opportunities for terrain passability in this region.

2.2. Input data

The input data, which form the basis for the MCDM analysis, are derived from various sources and encompass several critical aspects of the geographical and infrastructural landscape. These include the rivers, roads, rails, CORINE Land Cover (CLC), soil, and Digital Terrain Model (DTM) derived inputs such as slope and the TRI.

2.2.1. River, road, and rail network

River, road, and rail network data are obtained and adapted from the ©OpenStreetMap contributors dataset. This collaborative project provides freely available

2.2.4. DTM-derived inputs

The European DEM (EU-DEM; version 1.1 with free, full and open access to this data set; EEA, 2016) used in this study is the first homogenous DEM for the entire Europe, part of the Copernicus programme. This hybrid product, aimed at enhancing environmental management and addressing climate change, is derived from SRTM and ASTER GDEM data and fused by weighted averaging. Divided into 1-degree tiles and with a spatial resolution of approximately 30 meters, it facilitates detailed studies (EEA, 2016). The DEM is processed and enhanced by interpolation to 10 × 10 m spatial resolution using the QGIS 3.28 software package, a free and open-source cross-platform desktop GIS (QGIS Development Team, 2022). This software enables the visualization, processing, and analysis of geospatial data. Based on the enhanced EU-DEM data, it calculates the terrain's slope and TRI.

The slope, or incline, is vital to road design, referring to the surface's steepness, which affects stability and safety. High slopes can risk landslides and erosion, especially in unstable soil areas, necessitating slope stability analysis for infrastructure safety (Clayton, 1983). Slope angle also influences vehicle traversal difficulty, making understanding it essential for transportation planning and vehicle mobility studies. The slope is calculated using QGIS software version 3.28 (QGIS Development Team, 2022), precisely the GDALDEM slope function, employing Horn's formula (Horn, 1981; Rouault et al., 2023). This method derives the slope and aspect in a raster from a DEM (Equation 1; Horn, 1981):

$$\text{Slope} = \text{atan}\{\sqrt{[(dz/dx)^2 + (dz/dy)^2]}\} \quad (1)$$

where dz/dx and dz/dy are the changes in the z -value (elevation) over the changes in the x and y directions, respectively, and the atan function is the arctangent.

The TRI is used to quantify the elevation difference between adjacent cells of a DEM. It is a critical factor in understanding the complexity of a terrain's surface. The TRI is calculated by taking the square root of the sum of the squared differences between the elevation of each cell and the mean elevation of its eight surrounding cells (Equation 2; Riley et al., 1999):

$$\text{TRI} = \sqrt{\{[\sum (Z_{ij} - Z_{00})^2] / n\}} \quad (2)$$

where Z_{ij} represents the elevation of each neighbour cell, Z_{00} denotes the central cell, and n is the number of neighbour cells.

This measure provides a numerical representation of the terrain's roughness, which can significantly impact terrain passability. For instance, areas with high TRI values indicate rugged terrains that may be challenging for vehicles to traverse. In contrast, low TRI values suggest smoother terrains that may be more easily navigable (Habib, 2021).

2.3. MCDM weighted coefficients definition

This subsection overviews the weighted coefficients in the MCDM analysis. These coefficients are integral to the analysis as they assign quantitative values to the input data, thereby determining the relative importance of each criterion in the decision-making process. Estimating layer weights, precisely the weighted coefficients in the MCDM analysis is a detailed procedure involving several steps. The assignment of these coefficients is grounded in expert knowledge and undergoes sensitivity analysis to ensure the robustness of the results.

2.3.1. River network coefficients definition

The river network coefficients clarify the weighted coefficient assigned to the river network data. This coefficient reflects the influence of the river network on terrain passability, with

Table 1. Passability coefficients for river classes and different road categories

River class	Passability coefficient	Road categories*	Passability coefficient
1	100%	Railway	100%
2	80%	Motorway	100%
3	40%	Primary	100%
4	10%	Secondary	80%
5	5%	Tertiary	60%
6	2%	Unclassified	80%
7	0%	/	/
8 (bridge)	100%	/	/

Note. *Road categories are obtained from *Key:highway*, by OpenStreetMap Wiki, 2023 (<https://wiki.openstreetmap.org/wiki/Key:highway#Roads>). CC BY-SA 2.0.

higher values indicating a more significant impact. The coefficients for the river network passability are determined based on river classes, which are classified according to the Strahler stream order utilizing the Hy2roresO plugin (Gonnaud et al., 2019) in QGIS software. The Strahler stream order is a hierarchical classification system for rivers based on the connectivity and hierarchy of branching. Arthur Newell Strahler first proposed this system in the 1950s (Strahler, 1957), and it has

been widely used in hydrology and geomorphology to study river networks (Gleyzer et al., 2004). A total of seven classes are identified for the river network. The rivers' raster also includes bridges that intersect the watercourse, representing locations where vehicles can cross the water surface unimpeded (Table 1).

River class 1 is deemed fully passable with a 100% coefficient, representing easily fordable rivers with minimal vehicle movement challenges. River classes 2 through 4 are assigned decreasing passability coefficients (80%, 40%, 10%), reflecting moderate to challenging crossing conditions due to factors like depth and current speed. River classes 5 to 7 receive very low to zero coefficients (5%, 2%, 0%), indicating significant crossing difficulties or impossibility without bridges, while bridges are allocated with a 100% passability coefficient.

2.3.2. Road and rail network coefficients definition

The road and rail network coefficients detail the weighted coefficient assigned to the road and rail network data. This coefficient signifies the impact of the road and rail network on terrain passability, with higher values indicating a more significant influence (Table 1). Railways, motorways, and primary roads are assigned a 100% passability coefficient, reflecting their high maintenance, traffic volume handling, and minimal vehicle movement challenges. Secondary and unclassified roads have an 80% coefficient, indicating slightly reduced passability due to maintenance and surface quality variations. Tertiary roads are allocated a 60% coefficient, signifying further reduced passability, often caused by narrower lanes and less frequent maintenance.

2.3.3. Land cover coefficients definition

The land cover coefficients describe the weighted coefficient assigned to the land cover data. This coefficient represents the effect of different land cover types on terrain passability, with higher values indicating a more significant impact (Table 2).

Codes 211, 231, 242, and 321 are allocated a 100% passability coefficient, denoting flat and unobstructed terrains ideal for vehicle movement. Codes 334, 333, 243, 142, 324, and 332 receive reduced coefficients of 80% and 60%, indicating varying degrees of challenges such as uneven terrain or dense vegetation. The most challenging terrains, with codes 222, 311, 312, 313, 112, 512, 131, 121, and 133, are assigned coefficients ranging from 30% to 10%, reflecting significant obstructions like buildings, water bodies, or rough terrain, as categorized by the CLC system.

Table 2. Passability coefficients for different CLC classes

CLC*	Passability coefficient
211, 231, 242, 321	100%
334, 333, 243	80%
142, 324, 332	60%
222, 311, 312, 313	30%
112, 512, 131, 121, 133	10%

Note. *211 = Non-irrigated arable land, 231 = Pastures, 242 = Complex cultivation patterns, 321 = Natural grasslands, 334 = Burnt areas, 333 = Sparsely vegetated areas, 243 = Land principally occupied by agriculture, with significant areas of natural vegetation, 142 = Sport and leisure facilities, 324 = Transitional woodland-shrub, 332 = Bare rock, 222 = Fruit trees and berry plantations, 311 = Broad-leaved forest, 312 = Coniferous forest, 313 = Mixed forest, 112 = Discontinuous urban fabric, 512 = Water bodies, 131 = Industrial or commercial units, 121 = Industrial, commercial and transport units, 133 = Construction sites.

2.3.4. Soil coefficients definition

Soil passability ratings are influenced by terrain slope, soil texture, water presence, and weather conditions. In terrain passability, dry soil tends to be more compact and stable, allowing for easier traversal, while wet soil becomes slippery and less stable. A steep slope or high clay content can exacerbate the traversal difficulty. Therefore, understanding dry and wet periods is essential when assessing terrain passability through different soil types.

Soils can be classified into five primary types: gravel, sand, silt, clay, and organic matter. Gravel segments range in diameter from around 0.6 to 7.6 cm and are negligibly affected by weather, allowing vehicle traversal. Sand segments can be coarse, medium, or fine, and well-graded angular sand remains unaffected by frost or moisture. Silt, composed of natural rock particles, has good dry season passability, but becomes deep, impassable mud when wet. Clay consists of microscopic segments, providing a hard surface with excellent passability when dry, but becoming slippery and sticky when wet. Organic matter, such as organic mud and peat, exhibits medium to high compressibility and is identifiable by colour, smell, and spongy characteristics. These types may occur separately or in mixtures, with some of them being suitable for passability, making soil classification vital for practical terrain analysis (Rybansky, 2015).

Soil types, classified under the Standard Classification of Soils, are vital in determining vehicle movement across terrains. The pedological structure affects the speed and efficiency of travel, with surface deceleration coefficients differing for soil characters. For example, plane soil has a coefficient of 1.00, while stony soil ranges between 0.80 and 0.90. Specific soil types like gravel, sand, silt, clay, and organic matter present varying trafficability levels. Well-graded angular sand offers excellent trafficability, unaffected by frost or moisture, but dry, loose sand can hinder movement on slopes (Gigović et al., 2015; Rybansky, 2015).

The soil coefficients outline the weighted coefficient assigned to the soil data. This coefficient signifies the influence of soil characteristics on terrain passability, with higher values indicating a more significant effect. Soil types with the same passability coefficients are grouped to reduce Table 3 size.

Table 3. Terrain passability coefficients for various soil types during dry and wet periods

Soil group number	Passability coefficient (dry)	Passability coefficient (wet)	Soil group number	Passability coefficient (dry)	Passability coefficient (wet)
1	90	70	16	60	40
2	90	60	17	60	30
3	90	50	18	60	25
4	85	55	19	55	35
5	80	65	20	55	25
6	75	50	21	50	30
7	75	45	22	50	25
8	70	50	23	50	20
9	70	40	24	45	15
10	70	30	25	40	20
11	65	50	26	40	10
12	65	45	27	30	10
13	65	40	28	30	0
14	65	35	29	25	0
15	65	30	/	/	/

Note. Soil group number and soil types: 1 = Rendzina, carbonate, less eroded; 2 = Rendzina, carbonate, regolithic; 3 = Rendzina, carbonate, slightly skeletal, moderately eroded; 4 = Rendzina, carbonate, moderately skeletal, moderately eroded; 5 = Rendzina, carbonate, moderately skeletal, more eroded; 6 = Rendzina, carbonate, regolithic, moderately eroded; 7 = Rendzina, intercalated, slightly skeletal; Rendzina, intercalated, moderately eroded; 8 = Rendzina, intercalated, more eroded; Humus-silicate soil (ranker), eutrophic, slightly skeletal, moderately eroded; Humus-silicate soil (ranker), eutrophic intercalated moderately eroded; Humus-silicate soil (ranker), distric, slightly skeletal, moderately eroded; Humus-silicate soil (ranker), distric, slightly skeletal, more eroded; Humus-silicate soil (ranker), distric, moderately skeletal, skeletal, moderately eroded; Humus-silicate soil (ranker), distric, moderately skeletal, more eroded; Humus-silicate soil (ranker), distric, very skeletal, more eroded; Humus-silicate soil (ranker), distric, intercalated, moderately eroded; Humus-silicate soil (ranker), distric, lithic, more eroded; Vertisol, carbonate, moderately deep; Vertisol, carbonate, shallow; Vertisol, non-carbonate, deep; Vertisol, non-carbonate, shallow; 9 = Vertisol, intercalated, moderately deep; Lithosol, more eroded, rocky; Lithosol, moderately eroded, rocky; Regosol, silicate-carbonate, moderately eroded; 10 = Regosol, silicate, moderately eroded; 11 = Regosol, silicate, more eroded; 12 = Regosol, silicate-eutric, more eroded; 13 = Regosol, very skeletal, more eroded; 14 = Colluvial soil (colluvium), carbonate, with a predominance of soil material, loamy-clayey; Colluvial soil (colluvium), carbonate, with a predominance of fragments, slightly skeletal; Colluvial soil (colluvium), carbonate, with a predominance of soil material, slightly skeletal; 15 = Colluvial soil (colluvium), distric-silicate, alluvial-colluvial origin, moderately skeletal; 16 = Limestone-dolomite black soil (kalkomelanosol), organomineral, skeletal-colluvial, moderately eroded; Limestone-dolomite black soil (kalkomelanosol), organomineral, skeletal-colluvial, more eroded; Eutric cambisol, typical, less eroded; 17 = Eutric cambisol, typical, moderately eroded; Eutric cambisol, typical, slightly skeletal, less eroded; Eutric cambisol, typical, slightly skeletal, moderately eroded; Eutric cambisol, typical, slightly skeletal, more eroded; Eutric cambisol, vertic, less eroded; Eutric cambisol, lithic, moderately skeletal; 18 = Eutric cambisol, lithic, slightly skeletal, moderately eroded; 19 = Eutric cambisol, regolithic, moderately eroded; Distric cambisol, typical, moderately eroded; 20 = Distric cambisol, typical, slightly skeletal, moderately eroded; Calcocambisol, typical, moderately eroded; 21 = Luvisol, typical, less eroded; Fluvisol, carbonate, sandy-loamy; Fluvisol, carbonate, sandy-loamy; 22 = Fluvisol, carbonate, clayey-loamy; Fluvisol, carbonate, clayey; 23 = Fluvisol, carbonate gleyed, loamy; Fluvisol, non-carbonate, sandy-loamy; Fluvisol, non-carbonate, gravelly-sandy; Fluvisol, non-carbonate,

clayey-loamy; 24 = Pseudogley, on plateau, eutric, moderately deep; 25 = Pseudogley, on slope, eutric, moderately deep; 26 = Pseudogley, on slope, distric, shallow; 27 = Fluvial meadow soil (humofluvisol), non-carbonate, clayey; Fluvial meadow soil (humofluvisol), non-carbonate, moderately deep gleyed; 28 = Marsh black soil (humogley), non-carbonate, clayey; 29 = Swampy gley (eugley), amfigley, non-carbonate.

2.3.5. Slope coefficients definition

The slope coefficients provide information on the weighted coefficient assigned to the slope data. This coefficient reflects the impact of slope on terrain passability, with higher values indicating a more significant influence (Table 4). The selection of coefficients is based on a detailed consideration of terrain classifications concerning terrain slope, as presented in Borisov et al. (2011) and Živanović (2015). This selection of coefficients allows for a better understanding and interpretation of the terrain, which is vital for various applications, including assessing passability and overall terrain vulnerability.

Table 4. Passability coefficients for different slope categories

Slope	Passability coefficient	Terrain impact description
0–5°	100%	Flat or nearly flat terrain, allowing for maximum passability
5–10°	90%	Slightly inclined terrain may pose minimal challenges to vehicle movement but is generally passable
10–30°	80%	Moderate slopes can introduce more significant challenges, especially for heavy vehicles or those without specialised traction systems
30–40°	10%	Steeper slopes in this range may require specialised vehicles or equipment
40–60°	0%	Extremely steep terrains are often impassable for standard vehicles
>60°	0%	

2.3.6. TRI coefficients definition

The TRI coefficients detail the weighted coefficient assigned to the TRI data (Table 5). This coefficient represents the effect of topographic ruggedness on terrain passability, with higher values indicating a more significant impact.

TRI passability coefficients are derived from the TRI and Vehicle Movement Difficulty table (Hošková-Mayerová et al., 2020) and the obtained TRI values for the study area. The TRI is instrumental in this research, measuring surface complexity and offering insights into terrain navigability. High TRI values signify challenging terrains for vehicles, while low values indicate more passable landscapes. TRI's understanding aids in transportation planning and vehicle mobility studies, contributing to the MCDM analysis and enriching the research's scope. It links topographic ruggedness with terrain passability, resulting in a final terrain passability grid map. Overall, TRI is a strategic selection, providing a comprehensive perspective on terrain passability challenges aligning with the study's primary goals. Estimating layer weights involves a multi-faceted approach, incorporating expert knowledge, sensitivity analysis, and a detailed review of the existing

Table 5. TRI passability coefficient

TRI	Passability coefficient
0–2	100%
2–3	90%
3–5	70%
5–7	30%
7–10	10%
>10	0%

literature and studies. This approach ensures that the weighted coefficients are accurate and robust, enhancing the MCDM analysis's reliability.

3. Results

Table 6 presents a detailed comparison between river classes, defined by the Strahler order, and the distribution of bridges, roads, and railways within a specific region. The river classes range from 1 to 7, with a total length of 710.45 km and an additional bridge category of 13.05 km. On the other hand, the road categories are divided into Motorway, Primary, Secondary, Tertiary, and Unclassified, with a total road length of 1,359.29 km. Additionally, the railway length is provided at 84.84 km. This table offers valuable insights into the relationship between the infrastructure network and the natural river system. It can be instrumental in understanding the interplay between natural water bodies and human-made structures, potentially guiding urban planning, environmental conservation, and infrastructure development strategies.

Table 6. Overview of river classes by Strahler order, bridge distribution and road and railway lengths

River class by Strahler order and bridges	Length (km)	Road categories and railway	Length (km)
1	302.46	Motorway	133.89
2	114.65	Primary	48.56
3	144.10	Secondary	231.71
4	41.23	Tertiary	91.47
5	21.78	Unclassified	853.65
6	21.97	Total roads	1,359.29
7	64.26	Railway	84.84
Total rivers	710.45		
8 (bridges)	13.05		

Table 7 comprehensively overviews CLC class distribution across a study area. It is evident from the data that the most extensive land cover class is 311, covering an area of approximately 840.97 km². This is followed by 243 and 324 classes, covering 217.21 km² and 415.91 km², respectively. The least represented classes are 131, 133, and 334. The total area under consideration is 2,009.2 km². These findings provide valuable insights into land use patterns and could inform land management and conservation strategies.

Table 7. Distribution of CLC classes across a study area (in km²)

CLC class code	CLC class name	Area (km ²)
112	Discontinuous urban fabric	23.41
121	Industrial or commercial units	2.05
131	Mineral extraction sites	0.35
133	Construction sites	0.74
142	Sport and leisure facilities	0.49
211	Non-irrigated arable land	105.91
222	Fruit trees and berry plantations	1.14
231	Pastures	48.48
242	Complex cultivation patterns	188.24
	Land principally occupied by agriculture, with significant areas of	217.21
243	natural vegetation	
311	Broad-leaved forest	840.97

Table 7. Distribution of CLC classes across a study area (in km²; *continued*)

CLC class code	CLC class name	Area (km ²)
312	Coniferous forest	7.91
313	Mixed forest	21.82
321	Natural grasslands	120.04
324	Transitional woodland-shrub	415.91
332	Bare rocks	1.13
333	Sparsely vegetated areas	8.01
334	Burnt areas	2.38
512	Water bodies	2.97
	Total area	2,009.2

Table 8 presents the distribution of 29 soil groups across a study area of 2,009.2 km². The data reveals significant variation, with soil group 8 covering the most extensive area at 437.89 km² and soil group 15 the smallest at 0.12 km². This distribution underscores the complex and varied terrain within the study area. The findings highlight the dominance of certain soil groups and the presence of others in minimal areas, reflecting the heterogeneity of the landscape, with potential implications for various applications in the field of terrain analysis and vehicle passability.

Table 8. Distribution of different soil types across a study area (in km²)

Soil group No.	Area (km ²)	Soil group No.	Area (km ²)	Soil group No.	Area (km ²)
1	1.42	11	107.13	21	49.27
2	23.18	12	5.74	22	27.11
3	109.57	13	16.79	23	51.16
4	15.10	14	112.26	24	21.60
5	39.95	15	0.12	25	16.82
6	21.72	16	221.34	26	2.02
7	2.71	17	209.59	27	11.32
8	437.89	18	2.20	28	4.34
9	351.20	19	55.85	29	2.92
10	2.76	20	86.14	Total	2,009.2

The relationship between varying moisture conditions and the area's physical attributes, such as soil composition, land cover, and infrastructure, is vital in assessing terrain passability. Wet periods may render certain soils prone to erosion or water saturation, impacting road stability. Different land cover categories, like forests or farmlands, may also react distinctively to moisture levels, affecting terrain accessibility. Infrastructure quality and design must account for these fluctuating conditions to maintain resilience. Figure 3 offers insights into spatial distribution under diverse moisture scenarios, pinpointing areas susceptible to accessibility challenges due to weather factors around the City of Pirot. These maps are instrumental in guiding the MCDM process in urban planning, infrastructure, and environmental protection, reflecting the transportation network's resilience and adaptability to climatic changes.

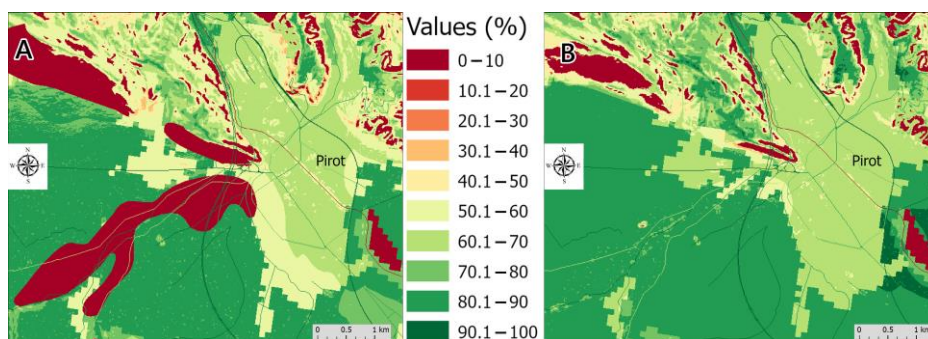


Figure 3. Terrain passability map for wet (A) and dry (B) period for the City of Pirot area.

Table 9 presents a comparative analysis of terrain passability maps, focusing on the area distribution across percentage ranges for wet and dry periods. The data is segmented into specific percentage ranges, and the corresponding areas (in km²) and percentages of the total area are provided for both climatic conditions. Table 9 illustrates a clear shift in terrain passability from the wet to the dry period. Lower percentage ranges are more prominent during wet conditions, while higher percentage ranges become more frequent during dry conditions. Within the lower percentage ranges (0–50), the wet period shows a higher total area (889.56 km² or 44.28%) compared to the dry period (679.04 km² or 33.80%). These values suggest that more areas are less passable during wet conditions. In the higher percentage ranges (50.1–100), conversely, the dry period exhibits a greater total area (1,330.14 km² or 66.20%) compared to the wet period (1,119.62 km² or 55.73%). These values indicate that more areas become highly passable during dry conditions. Within specific ranges, noticeable differences can be observed. For example, the 30.1–40% range shows a significant decrease from the wet (69.39 km² or 3.45%) to the dry period (10.68 km² or 0.53%). Similarly, the 90.1–100% range increases from the wet (3.86 km² or 0.19%) to the dry period (78.15 km² or 3.88%). These findings provide valuable insights into the region's transportation dynamics and can inform planning and decision-making processes to enhance transportation resilience and efficiency.

Table 9. Comparative overview of terrain passability maps area distribution (in km²) across percentage ranges for wet and dry periods

Ranges for the wet period (%)	Wet period area (km ²)	Wet period (%)	Ranges for the dry period (%)	Dry period area (km ²)	Dry period (%)
0–10	491.50	24.463	0–10	455.36	22.663
10.1–20	0.03	0.001	10.1–20	0.02	0.001
20.1–30	0.20	0.010	20.1–30	0.15	0.007
30.1–40	69.39	3.453	30.1–40	10.68	0.531
40.1–50	328.45	16.347	40.1–50	212.85	10.594
0–50 sum	889.56	44.275	0–50 sum	679.04	33.797
50.1–60	345.65	17.204	50.1–60	333.97	16.623
60.1–70	315.38	15.697	60.1–70	364.72	18.152
70.1–80	258.26	12.854	70.1–80	254.65	12.674
80.1–90	196.47	9.779	80.1–90	298.66	14.865
90.1–100	3.86	0.192	90.1–100	78.15	3.889
50.1–100 sum	1,119.62	55.725	50.1–100 sum	1,330.14	66.203

Figure 4 represents a raster grid analysis of a 1×1 km area encompassing 2,040 grid cells. This figure illustrates the summarised mean coefficient values for terrain passability maps during wet and dry periods for a 1 km^2 cell. The data reveals variations in passability across different cells, reflecting the spatial heterogeneity of the terrain. The relationship between the wet and dry period mean values may indicate the influence of seasonal changes on vehicle mobility, with specific cells showing significant differences between these periods. This quantitative analysis of geospace provides valuable insights into the valorised space, aiding in understanding the terrain's suitability for vehicular movement.

The detailed analysis presented in this section offers a complex view of the study area, encompassing aspects such as river classes, road categories, land cover, soil types, and terrain passability under varying moisture conditions. The findings indicate that the interaction between these elements is complex and significant in understanding the region's suitability for vehicular movement. Insights into the relationship between infrastructure and natural water bodies, land use patterns, soil composition, and climatic variations provide a comprehensive understanding that may guide urban planning, environmental conservation, infrastructure development, and transportation resilience. The spatial distribution of terrain passability, as illustrated through the comparative overview of wet and dry periods, further emphasises the dynamic nature of the terrain, setting the stage for an informed exploration of terrain analysis and vehicle passability.

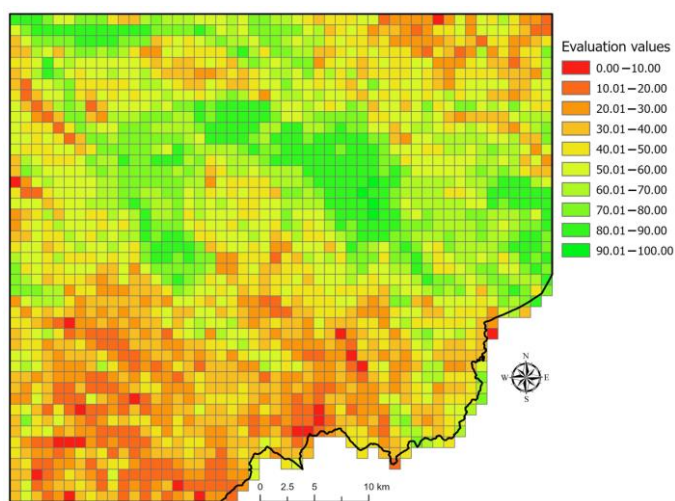


Figure 4. Terrain passability MCDM grid map.

4. Discussion

This research presents an in-depth comparative analysis of terrain passability maps, focusing on the distribution of areas across percentage ranges for wet and dry periods to understand the influence of climatic conditions on terrain passability. The lower percentage ranges (0–50 sum in Table 9) reveal more challenging areas for vehicle movement during the wet period (889.56 km^2 or 44.275%) than the dry period (679.04 km^2 or 33.797%), likely due to water-related obstacles. On the other hand, the higher percentage ranges (50.1–100 sum in Table 9) show more passable areas during the dry period (1,330.14 km^2 or 66.203%) than the wet period

(1,119.62 km² or 55.725%), possibly due to surface hardening. These findings suggest the need for alternative routes and support during wet conditions, while the dry period may allow for more flexible planning and faster travel. The data emphasize the terrain's sensitivity to moisture, as evidenced by the decrease in the 30.1–40% range from wet to dry and the increase in the 90.1–100% range. Table 9 highlights the terrain's dynamic nature across climatic conditions, offering vital insights for transportation authorities, urban planners, and emergency responders to enhance resilience, efficiency, and safety. Additionally, the study's use of the TRI index marks a significant advancement in topographic analysis and terrain passability, providing a more nuanced understanding of the terrain and distinguishing this work from others in the field.

This study, when compared to Borisov et al. (2011), not only demonstrates a focus on terrain and vehicle passability using GIS and MCDM analysis, but it also uniquely introduces the TRI and a detailed examination of wet and dry periods in southeastern Serbia, marking a substantial advancement. In contrast to Dawid and Pokonieczny (2021), our study offers a more comprehensive approach to terrain navigation, enhancing scholarly understanding and practical transportation planning. The comparison of our research with Hošková-Mayerová et al. (2020) highlights the diverse applications of spatial analysis, extending from transportation planning to theoretical methodology. While our research utilises GIS and MCDM analysis for environmental safety and disaster management, McCullough et al. (2017) focus on the NG-NRMM for vehicle mobility modelling, particularly in military contexts, reflecting the varied applications of mathematical modelling. The study by Rybansky et al. (2014), although exploring similar ideas, takes a different approach, with our paper providing a broader context, enriching the discourse on cross-country mobility. Finally, the comparison of our research with Stevens et al. (2017) emphasises the innovative use of GIS and terrain analysis in different fields, highlighting the potential for interdisciplinary collaboration and the broad impact of GIS in addressing real-world challenges.

The study presents a robust analysis of the production of terrain passability maps, emphasizing the dynamic nature of terrain passability across different climatic conditions. The introduction of the TRI and the comprehensive comparative analysis in Table 9 mark significant advancements in topographic analysis and terrain passability. The detailed examination of wet and dry periods offers critical insights for transportation planning, highlighting the sensitivity of certain terrains to moisture levels.

5. Conclusion

This study innovatively analyzes terrain passability maps in southeastern Serbia, employing an MCDM analysis and introducing the TRI. Exploring wet and dry periods marks a progression in understanding terrain passability. The findings reveal terrain sensitivity to moisture levels, offering insights into transportation planning, urban development, and environmental conservation. While the study's focus on southeastern Serbia may limit its applicability elsewhere, its contributions provide valuable insights into academic and practical fields. The study's unique approach enhances transportation resilience, efficiency, and safety, significantly advancing terrain passability understanding. However, the study has limitations regarding the specificity of river obstacle coefficients, such as depth, velocity, and bottom characteristics, and the absence of detailed soil properties like Consistency Index, Rigidity Index, Relative Compaction Index, and Vegetation Condition Index. Additionally, the study implements vegetation height via digital surface model, but does not incorporate detailed vegetation and forest structure metrics, such as tree spacing and Diameter at Breast Height values, which

could impact terrain passability. Future studies could broaden the geographical scope, integrate these more granular data points, and investigate additional influencing factors to further enrich the field's comprehension.

Acknowledgements

This paper is part of Project 1.22/2023 of the Ministry of Defense and the Serbian Army. This publication was prepared using the information from the European Union's Copernicus Land Monitoring Service.

References

- Antonović, G. M. (1982). *Pedološka karta SFRJ* [Pedological Map of SFRY]. Sheets Niš 4, Pirot 3 & 4, and Bosilegrad 1 & 2. Geokarta.
- Borisov, M. A., Banković, R. D., & Drobnjak, S. M. (2011). Evaluacija morfolometrijskih karakteristika zemljišta pri izradi karte tenkoprohodnosti [Evaluation of terrain geomorphometric characteristics for ground clearance charts production]. *Vojnotehnički glasnik*, 59(1), 62–80. <https://doi.org/10.5937/vojtehg1101062B>
- Clayton, J. L. (1983). Evaluating slope stability prior to road construction. United States Department of Agriculture, Forest Service, Intermountain Forest and Range Experiment Station. Research Paper, INT-307. <https://doi.org/10.2737/INT-RP-307>
- Dallas, J., Cole, M. P., Jayakumar, P., & Ersal, T. (2021). Terrain Adaptive Trajectory Planning and Tracking on Deformable Terrains. *IEEE Transactions on Vehicular Technology*, 70(11), 11255–11268. <https://doi.org/10.1109/TVT.2021.3114088>
- Dawid, W., & Pokonieczny, K. (2021). Methodology of Using Terrain Passability Maps for Planning the Movement of Troops and Navigation of Unmanned Ground Vehicles. *Sensors*, 21(14), Article 4682. <https://doi.org/10.3390/S21144682>
- Djouani, I., Dehimi, S., & Redjem, A. (2022). Evaluation of the efficiency and quality of the tram route of Setif city, Algeria: Combining AHP and GIS approaches. *Journal of the Geographical Institute "Jovan Cvijic" SASA*, 72(1), 85–102. <https://doi.org/10.2298/IJGI2201085D>
- Donlon, J. J., & Forbus, K. D. (1999, June 6–9). *Using a Geographic Information System for Qualitative Spatial Reasoning about Trafficability*. 13th International workshop on qualitative reasoning (QR99), Loch Awe, Scotland. https://www.qrg.northwestern.edu/papers/Files/Donlon_Forbus_QR99_Distribution.pdf
- Esri. (n.d.-a). *ArcGIS Pro* (Version 3.1.1) [Computer software]. ESRI Inc. <https://www.esri.com/en-us/arcgis/products/arcgis-pro/overview>
- Esri. (n.d.-b). *ArcGIS PRO help*. Esri. Retrieved September 11, 2023 from <https://pro.arcgis.com/en/pro-app/latest/help/main/welcome-to-the-arcgis-pro-app-help.htm>
- European Environment Agency. (2016). *European Digital Elevation Model (EU-DEM), version 1.1* [Data set]. <https://www.eea.europa.eu/en/datahub/datahubitem-view/d08852bc-7b5f-4835-a776-08362e2fbf4b>
- European Environment Agency geospatial data catalogue. (2020). *CORINE Land Cover 2018 (vector), Europe, 6-yearly - version 2020_20u1, May 2020* [Data set]. <https://doi.org/10.2909/71c95a07-e296-44fc-b22b-415f42acdf0>
- European Environment Agency. (2023, August 23). *Legal notice*. European Environment Agency. Retrieved October 28, 2023 from <https://www.eea.europa.eu/en/legal-notice#copyright-notice>
- Feranec, J., Soukup, T., Hazeu, G., & Jaffrain, G. (Eds.). (2016). *European Landscape Dynamics: CORINE Land Cover Data*. CRC Press. <https://doi.org/10.1201/9781315372860>
- Fisher, P. (1997). The pixel: A snare and a delusion. *International Journal of Remote Sensing*, 18(3), 679–685. <https://doi.org/10.1080/014311697219015>
- Gonnaud, A., Gaudin, M., & Vasseur, G. (2019). *Hy2roresO*. <https://hy2roreso.readthedocs.io/en/latest/>
- Gigović, Lj., Regodić, M., & Kostić, M. (2015). Integracija GIS-a i višekriterijumske tehnike u vrednovanju manevarske pogodnosti zemljišta [Integration of GIS and Multi-Criteria Techniques in Evaluating the Maneuverability Suitability of Land]. In N. Mladenović, D. Urošević, & Z. Stanimirović (Eds.),

- Proceedings of SYM-OP-IS 2015, 42nd International Symposium on Operations Research* (pp. 119–122). <http://symopis2015.matf.bg.ac.rs/ZbornikN.pdf>
- Gleyzer, A., Denisjuk, M., Rimmer, A., & Salingar, Y. (2004). A fast recursive GIS algorithm for computing Strahler stream order in braided and nonbraided networks. *Journal of the American Water Resources Association*, 40(4), 937–946. <https://doi.org/10.1111/j.1752-1688.2004.tb01057.x>
- Grabau, W. E. (1964). Terrain evaluation for mobility purposes. *Journal of Terramechanics*, 1(2), 22–32. [https://doi.org/10.1016/0022-4898\(64\)90062-X](https://doi.org/10.1016/0022-4898(64)90062-X)
- Graser, A., Asamer, J., & Ponweiser, W. (2015, June 3–5). *The elevation factor: Digital elevation model quality and sampling impacts on electric vehicle energy estimation errors*. 2015 International Conference on Models and Technologies for Intelligent Transportation Systems (MT-ITS), Budapest, Hungary. <https://doi.org/10.1109/MTITS.2015.7223240>
- Gumoš, A. K. (2005). *Modelling the Cross-Country Trafficability with Geographical Information Systems* (Master's thesis). Retrieved from <https://www.diva-portal.org/smash/get/diva2:20348/FULLTEXT01.pdf>
- Habib, M. (2021). Quantifying Topographic Ruggedness Using Principal Component Analysis. *Advances in Civil Engineering*, Article 3311912. <https://doi.org/10.1155/2021/3311912>
- Homer, C., Dewitz, J., Jin, S., Xian, G., Costello, C., Danielson, P., Gass, L., Funk, M., Wickham, J., Stehman, S., Auch, R., & Riitters, K. (2020). Conterminous United States land cover change patterns 2001–2016 from the 2016 National Land Cover Database. *ISPRS Journal of Photogrammetry and Remote Sensing*, 162, 184–199. <https://doi.org/10.1016/j.isprsjprs.2020.02.019>
- Horn, B. K. P. (1981). Hill shading and the reflectance map. *Proceedings of the IEEE*, 69(1), 14–47. <https://doi.org/10.1109/PROC.1981.11918>
- Hoškova-Mayerová, Š., Talhofer, V., Otrisal, P., & Rybanský, M. (2020). Influence of Weights of Geographical Factors on the Results of Multicriteria Analysis in Solving Spatial Analyses. *ISPRS International Journal of Geo-Information*, 9(8), Article 489. <https://doi.org/10.3390/ijgi9080489>
- House, M. L., Powers, W. L., Eisenhauer, D. E., Marx, D. B., & Fekersillassie, D. (2001). Spatial Analysis of Machine-Wheel Traffic Effects on Soil Physical Properties. *Soil Science Society of America Journal*, 65(5), 1376–1384. <https://doi.org/10.2136/sssaj2001.6551376x>
- Institut za zemljište Beograd. (2019). *Utvrdjivanje prirodnog fona pojedinih štetnih i opasnih materija u zemljištu na teritoriji Istočne Srbije* [Determining the natural background of certain harmful and hazardous substances in soil in the territory of Eastern Serbia]. <https://www.ekologija.gov.rs/sites/default/files/old-documents/Zemljište/Projekti/Prirodni-fon-stetnih-i-opasnih-materija-u-zemljištu-istocna-Srbija.pdf>
- Marković, J. Đ., & Pavlović, M. A. (1995). *Geografske regije Jugoslavije (Srbija i Crna Gora)* [Geographical regions of Yugoslavia (Serbia and Montenegro)]. Savremena administracija.
- McCullough, M., Jayakumar, P., Dasch, J., & Gorsich, D. (2017). The Next Generation NATO Reference mobility model development. *Journal of Terramechanics*, 73, 49–60. <https://doi.org/10.1016/j.jterra.2017.06.002>
- Okinda, F. W., Nyakach, S., & Nyaanga, D. M. (2021). Effect of tractor wheel traffic on selected soil physical properties. *Journal of Engineering in Agriculture and the Environment*, 7(2). <https://doi.org/10.37017/jae.v7i2.96>
- OpenStreetMap contributors. (2017). *Planet dump* [Data file from May 19, 2023]. Retrieved from <https://planet.openstreetmap.org>
- OpenStreetMap Wiki. (2023). *Key:highway*. OpenStreetMap Wiki. Retrieved May 20, 2023 from <https://wiki.openstreetmap.org/wiki/Key:highway#Roads>
- QGIS Development Team. (2022). *QGIS Geographic Information System* (Version 3.28) [Computer software]. QGIS Association. <http://qgis.org>
- Rada, J., Rybansky, M., & Dohnal, F. (2020). Influence of Quality of Remote Sensing Data on Vegetation Passability by Terrain Vehicles. *ISPRS International Journal of Geo-Information*, 9(11), Article 684. <https://doi.org/10.3390/ijgi9110684>
- Rada, J., Rybansky, M., & Dohnal, F. (2021). The Impact of the Accuracy of Terrain Surface Data on the Navigation of Off-Road Vehicles. *ISPRS International Journal of Geo-Information*, 10(3), Article 106. <https://doi.org/10.3390/ijgi10030106>

- Riley, S. J., DeGloria, S. D., & Elliot, R. (1999). A Terrain Ruggedness Index That Quantifies Topographic Heterogeneity. *Intermountain Journal of Sciences*, 5(1–4), 23–27. https://www.researchgate.net/publication/259011943_A_Terrain_Ruggedness_Index_that_Quantifies_Topographic_Heterogeneity
- Rouault, E., Warmerdam, F., Schwehr, K., Kiselev, A., Butler, H., Łoskot, M., Szekeres, T., Tourigny, E., Landa, M., Miara, I., Elliston, B., Chaitanya, K., Plesea, L., Morissette, D., Jolma, A., & Dawson, N. (2023). *GDAL* (Version v3.7.2) [Computer software]. Zenodo. <https://doi.org/10.5281/zenodo.8340595>
- Rybanský, M. (2003, August 10–16). *Effect of the Geographic Factors on the Cross Country Movement*. 21st International Cartographic Conference (ICC) "Cartographic Renaissance", Durban, South Africa. https://icaci.org/files/documents/ICC_proceedings/ICC2003/Papers/525.pdf
- Rybansky, M. (2015, May 19–21). *Soil trafficability analysis*. International Conference on Military Technologies (ICMT) 2015, Brno, Czech Republic. <https://doi.org/10.1109/MILTECHS.2015.7153728>
- Rybansky, M. (2022). Determination of Forest Structure from Remote Sensing Data for Modeling the Navigation of Rescue Vehicles. *Applied Sciences*, 12(8), Article 3939. <https://doi.org/10.3390/app12083939>
- Rybansky, M., Hofmann, A., Hubacek, M., Kovarik, V., & Talhofer, V. (2014, September 22–25). *The impact of terrain on cross-country mobility - Geographic factors and their characteristics*. 18th International Conference of the ISTVS, Seoul, Korea. https://www.researchgate.net/publication/276847750_The_Impact_of_Terrain_on_Cross-Country_Mobility_-_Geographic_Factors_and_their_Characteristics
- Rybansky, M., Kratochvil, V., Dohnal, F., Gerold, R., Kristalova, D., Stodola, P., & Nohel, J. (2023). GNSS Signal Quality in Forest Stands for Off-Road Vehicle Navigation. *Applied Sciences*, 13(10), Article 6142. <https://doi.org/10.3390/app13106142>
- Rybansky, M., & Rada, J. (2022). The Influence of the Quality of Digital Elevation Data on the Modelling of Terrain Vehicle Movement. *Applied Sciences*, 12(12), Article 6178. <https://doi.org/10.3390/app12126178>
- Saarilahti, M. (2002). *Soil interaction model*. <https://helda.helsinki.fi/server/api/core/bitstreams/722644c1-06a9-438e-855b-8cda339b5c99/content>
- Schulte, F., Zubert, T., Roeser, D., Meyer, N., & Kluge, T. (2021). A Real-Time-Capable Simulation Model for Off-Highway Applications Considering Soft Soil. *SAE International Journal of Commercial Vehicles*, 14(3), 351–364. <https://doi.org/10.4271/02-14-03-0029>
- Statistical Office of the Republic of Serbia. (2023). *Starost i pol. Podaci po naseljima* [Age and sex. Data by settlements]. <https://publikacije.stat.gov.rs/G2023/Pdf/G20234003.pdf>
- Stevens, M. T., McKinley, G. B., & Vahedifard, F. (2017). Full-featured ground vehicle mobility analysis using different soil moisture sources. *International Journal of Vehicle Performance*, 3(1), 19–35. <https://doi.org/10.1504/IJVP.2017.081262>
- Strahler, A. N. (1957). Quantitative analysis of watershed geomorphology. *Eos, Transactions American Geophysical Union*, 38(6), 913–920. <https://doi.org/10.1029/TR038i006p00913>
- Tobler, W. (1993). *Three Presentations on Geographical Analysis and Modeling: Non-Isotropic Geographic Modeling; Speculations on the Geometry of Geography; and Global Spatial Analysis* (Report No. 93–1). National Center for Geographic Information and Analysis. <https://escholarship.org/uc/item/05r820mz>
- Wollenstein-Betech, S., Houshmand, A., Salazar, M., Pavone, M., Cassandras, C. G., & Paschalidis, I. C. (2020, September 20–23). *Congestion-aware Routing and Rebalancing of Autonomous Mobility-on-Demand Systems in Mixed Traffic*. 2020 IEEE 23rd International Conference on Intelligent Transportation Systems (ITSC), Rhodes, Greece. <https://doi.org/10.1109/ITSC45102.2020.9294258>
- Živanović, S. (2015). Uticaj morfometrijskih parametara reljefa na rizik od šumskih požara [Influence morphometric parameters relief the risk of forest fire]. *Šumarstvo*, 67(4), 127–138. http://www.srpskosumarskoudruzenje.org.rs/pdf/sumarstvo/2015_4/sumarstvo2015_4_rad11.pdf